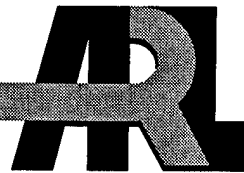


ARMY RESEARCH LABORATORY



Polarized Light Scattering from Irregular Contaminants on a Planar Substrate

Gorden Videen

ARL-TR-1727

October 1998

Reproduced From
Best Available Copy

19981201 011

Approved for public release; distribution unlimited.

100% QUALITY INSPECTED 3

The findings in this report are not to be construed as an official Department of the Army position unless so designated by other authorized documents.

Citation of manufacturer's or trade names does not constitute an official endorsement or approval of the use thereof.

Destroy this report when it is no longer needed. Do not return it to the originator.

Abstract

A model has been developed that can be used to predict the polarization state of scattered light from surface particles satisfying the specific criterion that the polarization state of the light scattered by the isolated particle is symmetric and resembles that of a Rayleigh sphere. Although this condition appears constraining, it may be satisfied by many common contaminants of interest, such as dust and aggregates of Rayleigh-sized particles. When these contaminants are placed on a substrate and the system is illuminated at near-grazing incidence, the polarization state of the scattered light is shown to be nearly independent of the actual shape and refractive index of the contaminant. It is, however, sensitive to the dimensions of the particle and substrate refractive index. Thus, the model may be useful in determining the size of surface contaminants.

Contents

1	Introduction	1
2	Model	3
3	Some Approximations	6
4	Conclusion	11
	References	12
	Distribution	15
	Report Documentation Page	17

Figures

1	Arizona road dust	2
2	Four non-zero normalized light-scattering Mueller matrix elements for symmetric scatterers shown for Arizona road dust measured at $\lambda = 0.4416 \mu\text{m}$	2
3	Geometry of scattering system, showing particle placed below substrate centered on coordinate system $j = 1$	4
4	Normalized polarization Mueller matrix elements calculated for a symmetric, irregular scatterer at $d = \lambda /4.7$ from a substrate ($n_{sub} = 0.5 - 3.5i$) illuminated at $\theta_o = 79^\circ$	10

1. Introduction

Many contaminants of interest are irregular particles, like dust and soot, which might be modeled as aggregates. Smoke particles, for instance, coagulate into sparse random clusters of Rayleigh-sized spherules. Although such clusters are large compared to the wavelength, their polarization Mueller matrix elements (S_{12} , S_{33} , and S_{34}) resemble those of a Rayleigh particle [1]. This similarity is also seen for complex structures like Arizona road dust, a sample of which is shown in figure 1. Mueller matrix elements for Arizona road dust have been measured with the polarization modulation techniques developed by Hunt and Huffman [2] and are compared to the elements of a Rayleigh sphere in figure 2. Even though the dust particles are many times larger than the wavelength, the polarization matrix elements have characteristics similar to those of the Rayleigh sphere: the characteristic dip in matrix element S_{12} , the characteristic S-shape of element S_{33} , and element $S_{34} \sim 0$. The evidence of the particle's size is contained within the total intensity element S_{11} . Rather than a symmetric intensity distribution with only a 50-percent dropoff at $\theta = 90^\circ$ (as would be expected for a Rayleigh sphere), we see a three-order-of-magnitude drop in intensity from the forward scatter, followed by an order-of-magnitude rise in intensity in the backscatter. Even though the total scattered intensity does not resemble that of a Rayleigh particle, the polarization elements strongly mimic Rayleigh scattering. I use this observation in developing a model of the polarization state of the light scattered from such particles placed on a substrate. Since irregular particles like dust and aggregates are common byproducts in many manufacturing processes, characterizing such particles is one of the motivating factors in developing such scattering models [3].

Figure 1. Arizona road dust.

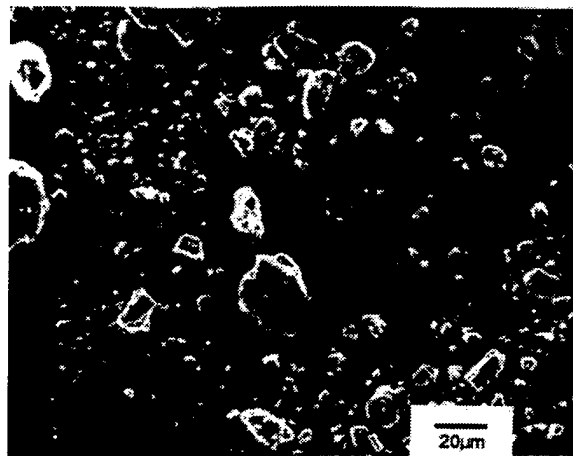
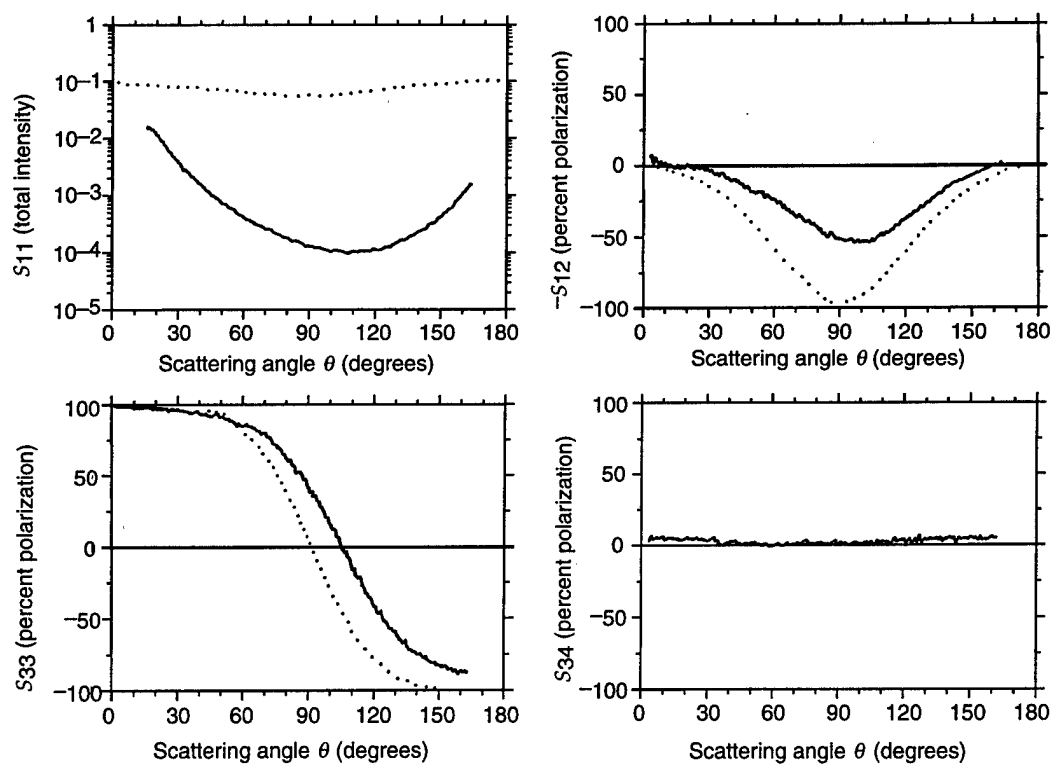


Figure 2. Four nonzero normalized light-scattering Mueller matrix elements for symmetric scatterers shown for Arizona road dust measured at $\lambda = 0.4416 \mu\text{m}$ (solid). Also shown are calculated normalized elements for a Rayleigh sphere (dots).



2. Model

One method of solving for the scattered fields from a particle near a plane interface is to use image theory. Figure 3 shows the geometry of the scattering system. A particle is placed a distance d beneath a plane interface separating a substrate of refractive index n_{sub} (above) from air (below). The incident, scattered, and interaction fields are each expressed as multipole expansions of vector spherical harmonics, and the boundary conditions at the surfaces of the particle and of the substrate are then satisfied simultaneously [4–8].

Consider expansions about the particle coordinate system ($j = 1$) and the image coordinate system ($j = 2$). These fields expanded about the particle coordinate system are

$$\mathbf{E}_{inc} = \sum_{n=0}^{\infty} \sum_{m=-n}^n a_{nm}^{(1)} \mathbf{M}_{nm,1}^{(1)} + a_{nm}^{(2)} \mathbf{N}_{nm,1}^{(1)}, \quad (1)$$

$$\mathbf{E}_{sca} = \sum_{n=0}^{\infty} \sum_{m=-n}^n b_{nm}^{(1)} \mathbf{M}_{nm,1}^{(3)} + b_{nm}^{(2)} \mathbf{N}_{nm,1}^{(3)}, \quad (2)$$

$$\mathbf{E}_{int} = \sum_{n=0}^{\infty} \sum_{m=-n}^n c_{nm}^{(1)} \mathbf{M}_{nm,1}^{(1)} + c_{nm}^{(2)} \mathbf{N}_{nm,1}^{(1)}, \quad (3)$$

where $\mathbf{M}_{nm,j}^{(i)}$ and $\mathbf{N}_{nm,j}^{(i)}$ are vector spherical harmonics expanded by Bessel functions of the i th kind expanded about the $j = 1$ coordinate system. The scattering solution can be found directly from the scattering response, or T-matrix, of the isolated particle to an incident wave of the form

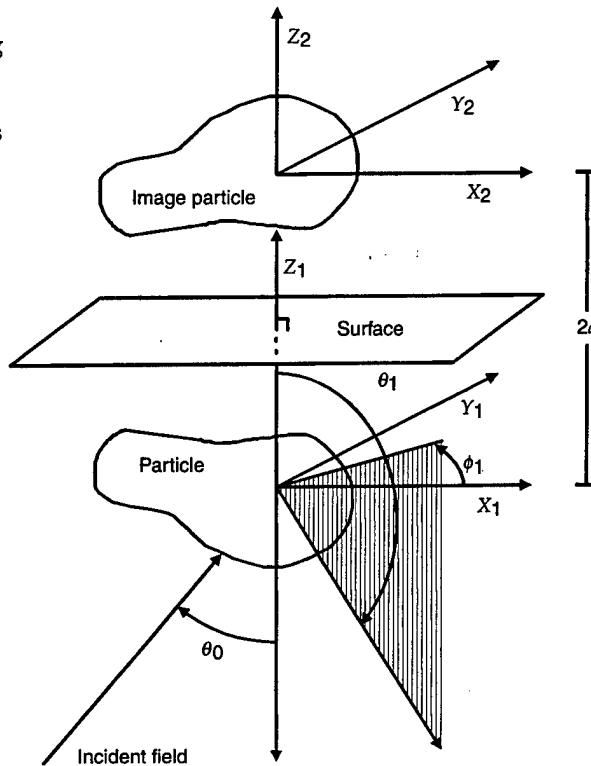
$$\mathbf{E}_{inc} = A_{nm}^{(1)} \mathbf{M}_{nm}^{(1)} + A_{pq}^{(2)} \mathbf{N}_{pq}^{(1)} \quad (4)$$

and is given by

$$\mathbf{E}_{sca} = \sum_{n',m'} A_{nm}^{(1)} B_{n'm'1}^{(n,m,1)} \mathbf{M}_{n'm'}^{(1)} + A_{nm}^{(1)} B_{n'm'2}^{(n,m,1)} \mathbf{N}_{n'm'}^{(1)} + A_{pq}^{(2)} B_{n'm'1}^{(p,q,2)} \mathbf{M}_{n'm'}^{(1)} + A_{pq}^{(2)} B_{n'm'2}^{(p,q,2)} \mathbf{N}_{n'm'}^{(1)}. \quad (5)$$

The solution to the scatter from an arbitrarily shaped particle placed near a plane interface has recently been formulated [7,8]. These results can easily be modified to accommodate substrates that are not perfectly

Figure 3. Geometry of scattering system, showing particle placed below substrate centered on coordinate system $j = 1$. Its image is centered above substrate on coordinate system $j = 2$.



conducting, with the following approximation: say the interaction field is the image of the scattered field from the particle that strikes the substrate at normal incidence before again interacting with the particle [4,6]. The interaction coefficients can then be expressed as

$$c_{nm}^{(1)} = R_{TE}(0) \sum_{n'} (-1)^{n'+m} \left[b_{n'm}^{(1)} D_n^{(n',m)} - b_{n'm}^{(2)} E_n^{(n',m)} \right], \quad (6)$$

$$c_{nm}^{(2)} = R_{TE}(0) \sum_{n'} (-1)^{n'+m} \left[b_{n'm}^{(1)} E_n^{(n',m)} - b_{n'm}^{(2)} D_n^{(n',m)} \right], \quad (7)$$

where $D_n^{(n',m)}$ and $E_n^{(n',m)}$ are translation coefficients used to translate vector spherical harmonics in the image coordinate system to vector spherical harmonics in the particle coordinate system:

$$\mathbf{M}_{n'm,2}^{(3)} = \sum_{n'} D_{n'}^{(n',m)} \mathbf{M}_{n'm,1}^{(1)} + E_{n'}^{(n',m)} \mathbf{N}_{n'm,1}^{(1)}, \quad (8)$$

$$\mathbf{N}_{n'm,2}^{(3)} = \sum_{n'} E_n^{(n',m)} \mathbf{M}_{n'm,1}^{(1)} + D_{n'}^{(n',m)} \mathbf{N}_{n'm,1}^{(1)}, \quad (9)$$

and $R_{T*}(\theta)$ are the standard Fresnel reflection coefficients for a plane wave reflecting off the substrate. The scattering coefficients are then

$$\begin{aligned}
b_{nm}^{(p)} = & \sum_{n'm'} B_{nmp}^{(n',m',1)} \left\{ a_{n'm'}^{(1)} + R_{TE}(0) \sum_q (-1)^{q+m'} \left[b_{qm'}^{(1)} D_n^{(q,m')} - b_{qm'}^{(2)} E_n^{(q,m')} \right] \right\} \\
& + B_{nmp}^{(n',m',2)} \left\{ a_{n'm'}^{(2)} + R_{TE}(0) \sum_q (-1)^{q+m'} \left[b_{qm'}^{(1)} E_n^{(q,m')} - b_{qm'}^{(2)} D_n^{(q,m')} \right] \right\}.
\end{aligned} \quad (10)$$

Adding the electric-field components emanating from the particle and its image yields the scattering amplitude matrix:

$$\begin{pmatrix} E_\theta^{sca} \\ E_\phi^{sca} \end{pmatrix} = \frac{\exp[ikr]}{-ikr} \begin{bmatrix} S_2 & S_3 \\ S_4 & S_1 \end{bmatrix} \begin{pmatrix} E_{TM}^{inc} \\ E_{TE}^{inc} \end{pmatrix} \quad (11)$$

where the scattered amplitudes are the superposition of the scattered fields from the object and the image:

$$\begin{aligned}
S_1 = & \sum_{nm} (-i)^n \exp(im\phi) \left\{ \left[1 + R_{TE}(\pi - \theta) (-1)^{n+m} \exp(-2ikd \cos \theta) \right] b_{nm}^{(2)TE} \frac{m \tilde{P}_n^m(\theta)}{\sin \theta} \right. \\
& \left. + \left[1 - R_{TE}(\pi - \theta) (-1)^{n+m} \exp(-2ikd \cos \theta) b_{nm}^{(1)TE} \frac{\partial}{\partial \theta} \tilde{P}_n^m(\theta) \right] \right\} \quad (12)
\end{aligned}$$

$$\begin{aligned}
S_2 = & \sum_{nm} (-i)^{n+1} \exp(im\phi) \left\{ \left[1 + R_{TM}(\pi - \theta) (-1)^{n+m} \exp(-2ikd \cos \theta) \right] b_{nm}^{(1)TM} \frac{m \tilde{P}_n^m(\theta)}{\sin \theta} \right. \\
& \left. + \left[1 - R_{TM}(\pi - \theta) (-1)^{n+m} \exp(-2ikd \cos \theta) b_{nm}^{(2)TM} \frac{\partial}{\partial \theta} \tilde{P}_n^m(\theta) \right] \right\} \quad (13)
\end{aligned}$$

$$\begin{aligned}
S_3 = & \sum_{nm} (-i)^{n+1} \exp(im\phi) \left\{ \left[1 + R_{TM}(\pi - \theta) (-1)^{n+m} \exp(-2ikd \cos \theta) \right] b_{nm}^{(1)TE} \frac{m \tilde{P}_n^m(\theta)}{\sin \theta} \right. \\
& \left. + \left[1 - R_{TM}(\pi - \theta) (-1)^{n+m} \exp(-2ikd \cos \theta) b_{nm}^{(2)TE} \frac{\partial}{\partial \theta} \tilde{P}_n^m(\theta) \right] \right\} \quad (14)
\end{aligned}$$

$$\begin{aligned}
S_4 = & \sum_{nm} (-i)^n \exp(im\phi) \left\{ \left[1 + R_{TE}(\pi - \theta) (-1)^{n+m} \exp(-2ikd \cos \theta) \right] b_{nm}^{(2)TM} \frac{m \tilde{P}_n^m(\theta)}{\sin \theta} \right. \\
& \left. + \left[1 - R_{TE}(\pi - \theta) (-1)^{n+m} \exp(-2ikd \cos \theta) b_{nm}^{(1)TM} \frac{\partial}{\partial \theta} \tilde{P}_n^m(\theta) \right] \right\}. \quad (15)
\end{aligned}$$

The incident field coefficients $b_{nm}^{(j)TE}$ and $b_{nm}^{(j)TM}$ in these expressions are for the superposition of the real and image TE and TM plane waves [4].

3. Some Approximations

The equations in the previous section may be used to calculate the scattered fields from a particle near a highly reflecting substrate. Their primary drawback is that numerically finding the scattering coefficients (eq (10)) requires a matrix inversion. Although such numerical calculations are achieved more cost-efficiently than are numerical techniques like discrete dipole approximation (DDA), they are still not conducive to the rapid calculations necessary for modeling surfaces produced in the manufacturing process. More importantly, when such operations are performed, much of the physical insight into a solution is lost.

In certain instances, the matrix is diagonal, and the solution is greatly simplified. If, for instance, the interaction field is small compared to the incident field, the off-diagonal elements of the matrix form of equation (10) are small compared with the diagonal elements, and $b_{nm}^{(p)} \sim B_{nmp}^{(n',m',1)} a_{n',m'}^{(1)}$. Such conditions obviously exist for Rayleigh and Rayleigh-Gans particles and particles placed a large distance from the substrate. The scattered field from a particle on a substrate can then be found directly as the superposition of the scattered fields from the particle and the image particle, without any consideration of the interaction. In the plane defined by the surface normal and the incident wavevector, the scattered field from a particle resting on a substrate can be expressed as the superposition of the fields from the particle and image particle; i.e., in the plane of incidence, equations (12) and (13) may be written as

$$\begin{aligned} S_1(\theta - \theta_o) = & S_1^o(\theta_o, \theta - \theta_o) + S_1^o(\pi - \theta_o, \theta + \theta_o - \pi) R_{TE}(\theta_o) \exp[i\delta(\theta_o, d)] \\ & + S_1^o(\theta_o, \pi - \theta - \theta_o) R_{TE}(\pi - \theta) \exp[i\delta(\pi - \theta, d)] \\ & + S_1^o(\pi - \theta_o, \theta_o - \theta) R_{TE}(\theta_o) R_{TE}(\pi - \theta) \exp\{i[\delta(\theta_o, d) + \delta(\pi - \theta, d)]\}, \end{aligned} \quad (16)$$

$$\begin{aligned} S_2(\theta - \theta_o) = & S_2^o(\theta_o, \theta - \theta_o) + S_2^o(\pi - \theta_o, \theta + \theta_o - \pi) R_{TM}(\theta_o) \exp[i\delta(\theta_o, d)] \\ & + S_2^o(\theta_o, \pi - \theta - \theta_o) R_{TM}(\pi - \theta) \exp[i\delta(\pi - \theta, d)] \\ & + S_2^o(\pi - \theta_o, \theta_o - \theta) R_{TM}(\theta_o) R_{TM}(\pi - \theta) \exp\{i[\delta(\theta_o, d) + \delta(\pi - \theta, d)]\}, \end{aligned} \quad (17)$$

where in the far field $\theta \sim \theta_1 \sim \theta_2$, $\delta(\theta, d) = 2kd \cos \theta$; also, $S_1(\theta_o, \theta - \theta_o)$ and $S_2(\theta_o, \theta - \theta_o)$ are the scattering amplitude matrix elements for the

isolated particle illuminated by a plane wave whose wavevector is oriented at angle θ_o with respect to the z -axis, and $\theta - \theta_o$ is the scattering angle measured from the specular direction. Equations (16) and (17) are a direct result of setting the interaction fields equal to zero in the equations describing the scatter from particles on or near substrates [4-12].

It is likely that the interaction fields will be negligible for some highly irregular particles resting on a substrate: e.g., particles consisting of aggregates of Rayleigh spheres. The polarization state of the scattered light from these isolated aggregates resembles that of a Rayleigh sphere; i.e., the particle acts as a group of individual, noninteracting Rayleigh subparticles, for which there is interference between the waves emanating from each subparticle but very little interaction between the subparticles [1]. Since there is negligible interaction between subparticles of the system, it can reasonably be assumed that there would also be negligible interaction between the particle and its image when it is placed on a substrate. The scattering amplitude matrix elements for an isolated Rayleigh scattering system are related by

$$S_2^o(\theta_o, \theta - \theta_o) = \cos(\theta - \theta_o) S_1^o(\theta_o, \theta - \theta_o). \quad (18)$$

This equation is also valid for a conglomeration of noninteracting Rayleigh spheres and is approximately valid for some highly irregular particles (e.g., the Arizona road dust of fig. 1 and 2). By using the Rayleigh-scattering approximation of equation (18), one can express $S_2^o(\theta_o, \theta - \theta_o)$ in terms of $S_1^o(\theta_o, \theta - \theta_o)$ in equations (16) and (17).

One final condition in developing this scattering model is that at some particle-coordinate-system location, the scattering amplitude matrix elements for the isolated particle are symmetric:

$$S_1^o(\theta_o, \theta - \theta_o) = S_1^o(\theta_o, \theta_o - \theta). \quad (19)$$

Such a condition is valid for symmetric particles such as spheres, ellipsoids, and dipoles when the coordinate system is at the center of the particle. In addition, we know that the scattering phase function (which is the sum of the magnitudes squared of the scattering amplitude matrix elements) of many particles is also approximately symmetric. The scattering amplitude matrix elements, however, contain the phase information of the scattered fields and are dependent on the placement of the particle coordinate system. For example, if we move the coordinate system close to one edge of a spherical scatterer, the complex amplitudes of the scattered spherical waves expressed in that coordinate system are no longer symmetric, even though the intensity distribution in the far field is quite symmetric.

For highly irregular systems, equation (19) may hold some validity at a coordinate system placed at some central location of the particle. The accuracy of using this approximation is further increased if we average the scattering amplitudes over some finite area to average out the high-frequency interference structure contained in the scattering amplitude coefficients. This is physically equivalent to having collection optics or a finite-size detector collect the scattered field. Although not all irregular particles would be expected to satisfy this condition, the comparison with experimental results given below shows that this condition is at least partially satisfied for some substrate contaminants.

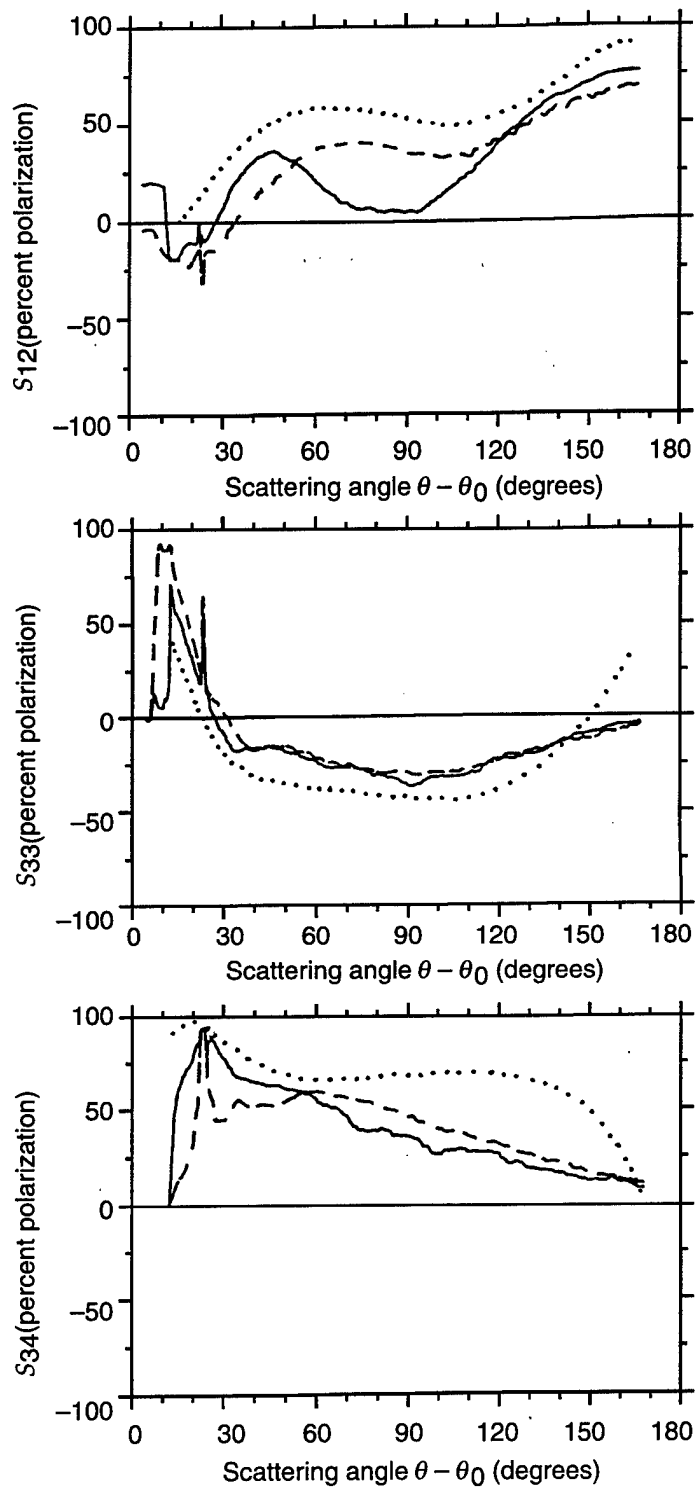
We can now derive the polarization state of scattered light for contaminants fulfilling the symmetric-scatterer (eq (19)) and the noninteracting-Rayleigh-scatterer (eq (18)) conditions. If the substrate is illuminated at near-grazing incidence ($\theta_o \sim \pm 90^\circ$), the scattering amplitudes of the isolated particle ($S_1^o(\theta_o, \theta - \theta_o)$ and $S_2^o(\theta_o, \theta - \theta_o)$) may be factored out of equations (16) and (17), and completely cancel from the normalized polarization matrix elements. The normalized polarization matrix elements now depend only on the separation distance d of the particle from the substrate, the substrate complex refractive index n_{sub} , and the incident angle θ_o (as long as $\theta_o \sim \pm 90^\circ$).

It is important to note that the separation parameter d is the distance from the surface of the substrate to some particle coordinate system location at which the symmetric-scatterer approximation holds. The physical extent of a symmetric scatterer is equal to $2d$, since this location must be at the center of such a particle. If the particle is not symmetric, we would still expect it to be located near some central location of the particle, so that the particle would have a physical dimension of approximately $2d$. With a particle of this size, we can now apply the model to determine the size of contaminants located on substrates by varying the separation distance (particle size) in the model until the polarization state of the scattered light matches the experimentally measured state. Finally, note that illuminating the system at grazing incidence also reduces the interaction term, since the large forward-scattering lobe is directed along the surface rather than back toward the particle.

To model the scattered light of contaminants on a substrate, let us compare model results with the normalized polarization Mueller matrix elements of select perfect and decayed optical substrates measured by Iafelice and Bickel [13]. These systems are Al-coated sapphire substrates with rms surface roughness $\sigma = 1.6 \pm 0.3$ nm. However, the authors note that surface defects consisting of residual particles ranging in size from ~ 0.2 to $1.0 \mu\text{m}$ sparsely littered both substrates. Although no difference in

size distribution was apparent, the decayed mirror surface had approximately five times as many defects as the perfect mirror surface. During the measurements, the laser light was focussed at several different locations on the substrate, and sites with large scattering were avoided; thus, it is likely that only one of the smaller scatterers was illuminated when measurements were taken. Figure 4 shows the Mueller matrix elements measured [13] at near-grazing incidence ($\theta_o = 79^\circ$) with $\lambda = 0.4416 \mu\text{m}$. Also shown are the calculated polarization matrix elements for a symmetric scatterer at a separation distance $d = \lambda/4.7$ from the ($n_{sub} = 0.5 + 3.5i$) substrate. Since the substrate refractive index is highly dependent on the thickness of the aluminum oxide layer that forms on the surface and acts as an anti-reflection coating, this value is reasonable. Values for pure Al are on the order of $n_{sub} = 0.5 + 5.0i$. Videen and Ngo [14] compared theoretical and experimental Mueller matrix elements of a cylinder resting on a substrate prepared by the same method as Iafelice and Bickel and found best fits for $n_{sub} = 0.5 + 3.8i$. The separation distance ($d = \lambda/4.7$) corresponds to particles having dimensions of $\sim 0.2 \mu\text{m}$ of the estimated size range. Overall, the fit of the model results to measurement is good. Model calculations of matrix element S_{12} bear a striking resemblance to those of the decayed mirror surface (increasing the separation distance slightly also produces the hump at $\theta - \theta_o \sim 85^\circ$ for the perfect mirror surface). The general shapes of measurement and model results for matrix elements S_{33} and S_{34} are also in good agreement.

Figure 4. Normalized polarization Mueller matrix elements calculated for a symmetric, irregular scatterer at $d = \lambda/4.7$ from a substrate ($n_{sub} = 0.5 - 3.5i$) illuminated at $\theta_o = 79^\circ$ (dots). Superimposed are experimental matrix elements measured by Iafelice and Bickel [13] of a perfect mirror surface (solid) and a decayed mirror surface (dashes), $\lambda = 0.4416 \mu\text{m}$.



4. Conclusion

A model has been developed that can be used to predict the polarization state of light scattered from irregular particles on a plane interface illuminated at near-grazing incidence. The model assumes that the interaction of the particle with its image is small compared with the illuminating field and that the scattered field from the isolated particle is symmetric in some particulate coordinate system. The polarization state of the scattered light is sensitive to the particle size (distance from the substrate to the particulate coordinate system) and the substrate refractive index, but is insensitive to the actual shape of the contaminant. Such a model is useful for sizing contaminants.

References

1. R. H. Zerull, B.Å.S. Gustafson, K. Schulz, and E. Thiele-Corbach: Scattering by aggregates with and without an absorbing mantle: Microwave analog experiments. *Appl. Opt.* **32** (1993), 4088–4100.
2. A. J. Hunt and D. R. Huffman: A new polarization-modulated light scattering instrument. *Rev. Sci. Instrum.* **44** (1973), 1753–1762.
3. G. Videen: Polarized light scattering from surface contaminants. *Opt. Commun.* **143** (1997), 173–178.
4. G. Videen: Light scattering from a sphere on or near a surface. *J. Opt. Soc. Am. A* **8** (1991), 483–489; Errata. *J. Opt. Soc. Am. A* **9** (1992), 844–845.
5. B. R. Johnson: Light scattering from a spherical particle on a conducting plane. *J. Opt. Soc. Am. A* **9** (1992), 1341–1351; Erratum. *J. Opt. Soc. Am. A* **10** (1993), 766.
6. B. R. Johnson: Calculation of light scattering from a spherical particle on a surface by the multipole expansion method. *J. Opt. Soc. Am. A* **13** (1996), 326–337.
7. G. Videen: Light scattering from a particle on or near a perfectly conducting surface. *Opt. Commun.* **115** (1995), 1–7.
8. F. Borghese, P. Denti, R. Saija, E. Fucile, and O. I. Sindoni: Optical properties of model anisotropic particles on or near a perfectly reflecting surface. *J. Opt. Soc. Am. A* **12** (1995), 530–540.
9. I. V. Lindell, A. H. Sihvola, K. O. Muinonen, and P. W. Barber: Scattering by a small object close to an interface. I. Exact-image theory formulation. *J. Opt. Soc. Am. A* **8** (1991), 472–476.
10. K. O. Muinonen, A. H. Sihvola, I. V. Lindell, and K. A. Lumme: Scattering by a small object close to an interface. II. Study of backscattering. *J. Opt. Soc. Am. A* **8** (1991), 477–482.
11. Y. Eremin and N. Orlov: Simulation of light scattering from a particle upon a wafer surface. *Appl. Opt.* **35** (1996), 6599–6604.

12. G. Videen, W. L. Wolfe, and W. S. Bickel: The light-scattering Mueller matrix for a surface contaminated by a single particle in the Rayleigh limit. *Opt. Eng.* **31** (1992), 341–349.
13. V. J. Iafelice and W. S. Bickel: Polarized light scattering matrix elements for select perfect and perturbed optical surfaces. *Appl. Opt.* **26** (1987), 2410–2415.
14. G. Videen and D. Ngo: Light scattering from a cylinder near a plane interface: Theory and comparison with experimental data. *J. Opt. Soc. Am. A* **14** (1997), 70–78.

Distribution

Admnstr Defns Techl Info Ctr Attn DTIC-OCP 8725 John J Kingman Rd Ste 0944 FT Belvoir VA 22060-6218	US Army NGIC Attn Rsrch & Data Branch 220 7th Stret NE Charlottesville VA 22901-5396
Dfns Intllgnc Acgy Attn DT 2 Wpns & Sys Div Washington DC 20301	US Army Nuc & Cheml Agency 7150 Heller Loop Ste 101 Springfield VA 22150-3198
Central Intllgnc Agency Dir DB Standard Attn GE 47 QB Washington DC 20505	US Army Strtgc Defns Cmnd Attn CSSD H MPL Techl Lib Attn CSSD H XM Dr Davies PO Box 1500 Huntsville AL 35807
Chairman Joint Chiefs of Staff Attn J5 R&D Div Washington DC 20301	US Military Academy Dept of Mathematical Sci Attn MAJ M D Engen West Point NY 10996
Dir of Defns Rsrch & Engrg Attn DD TWP Attn Engrg Washington DC 20301	Dept of the Navy Chief of Nav OPS Attn OP 03EG Washington DC 20350
Commanding Officer Attn NMCB23 6205 Stuart Rd Ste 101 FT Belvoir VA 22060-5275	DARPA Attn B Kaspar Attn Techl Lib 3701 N Fairfax Dr Arlington VA 22203-1714
Dir of Chem & Nuc Ops DA DCSOPS Attn Techl Lib Washington DC 20301	US Dept of Energy Attn KK 22 K Sisson Attn Techl Lib Washington DC 20585
Hdqtrs Dept of the Army Attn DAMO-FDT D Schmidt 400 Army Pentagon Rm 3C514 Washington DC 20301-0460	US Army Rsrch Lab Attn SLCRO-D PO Box 12211 Research Triangle Park NC 27709-2211
OIR CSB CRB Attn A M JOnes RB 1413 OHM Washington DC 20505	US Army Rsrch Lab Attn AMSRL-CI-LL Techl Lib (3 copies) Attn AMSRL-CS-AS Mail & Records Mgmt Attn AMSRL-CS-EA-TP Techl Pub (3 copies) Attn AMSRL-IS-EE G Videen (5 copies) Adelphi MD 20783-1197
US Army Engrg Div Attn HNDED FD PO Box 1500 Huntsville AL 35807	

REPORT DOCUMENTATION PAGE

*Form Approved
OMB No. 0704-0188*

Public reporting burden for this collection of information is estimated to average 1 hour per response, including the time for reviewing instructions, searching existing data sources, gathering and maintaining the data needed, and completing and reviewing the collection of information. Send comments regarding this burden estimate or any other aspect of this collection of information, including suggestions for reducing this burden, to Washington Headquarters Services, Directorate for Information Operations and Reports, 1215 Jefferson Davis Highway, Suite 1204, Arlington, VA 22202-4302, and to the Office of Management and Budget, Paperwork Reduction Project (0704-0188), Washington, DC 20503.

1. AGENCY USE ONLY <i>(Leave blank)</i>	2. REPORT DATE October 1998	3. REPORT TYPE AND DATES COVERED Final, October 1997 to June 1998	
4. TITLE AND SUBTITLE Polarized Light Scattering from Irregular Contaminants on a Planar Substrate		5. FUNDING NUMBERS DA PR: B53A PE: 61102A	
6. AUTHOR(S) Gorden Videen		8. PERFORMING ORGANIZATION REPORT NUMBER ARL-TR-1727	
7. PERFORMING ORGANIZATION NAME(S) AND ADDRESS(ES) U.S. Army Research Laboratory Attn: AMSRL-IS-EE 2800 Powder Mill Road Adelphi, MD 20783-1197			
9. SPONSORING/MONITORING AGENCY NAME(S) AND ADDRESS(ES) U.S. Army Research Laboratory 2800 Powder Mill Road Adelphi, MD 20783-1197		10. SPONSORING/MONITORING AGENCY REPORT NUMBER	
11. SUPPLEMENTARY NOTES ARL PR: 7FEJ70 AMS code: 61110253A11			
12a. DISTRIBUTION/AVAILABILITY STATEMENT Approved for public release; distribution unlimited.		12b. DISTRIBUTION CODE	
13. ABSTRACT <i>(Maximum 200 words)</i> A model has been developed that can be used to predict the polarization state of scattered light from surface particles satisfying the specific criterion that the polarization state of the light scattered by the isolated particle is symmetric and resembles that of a Rayleigh sphere. Although this condition appears constraining, it may be satisfied by many common contaminants of interest, such as dust and aggregates of Rayleigh-sized particles. When these contaminants are placed on a substrate and the system is illuminated at near-grazing incidence, the polarization state of the scattered light is shown to be nearly independent of the actual shape and refractive index of the contaminant. It is, however, sensitive to the dimensions of the particle and substrate refractive index. Thus, the model may be useful in determining the size of surface contaminants.			
14. SUBJECT TERMS Contaminants, Mueller matrix		15. NUMBER OF PAGES 23	
16. PRICE CODE			
17. SECURITY CLASSIFICATION OF REPORT Unclassified	18. SECURITY CLASSIFICATION OF THIS PAGE Unclassified	19. SECURITY CLASSIFICATION OF ABSTRACT Unclassified	20. LIMITATION OF ABSTRACT SAR